AJNR

Topological Structural Brain Connectivity Alterations in Aspartylglucosaminuria: A Case-Control Study

U. Roine, A.M. Tokola, T. Autti and T. Roine

AJNR Am J Neuroradiol 2023, 44 (1) 40-46
doi: https://doi.org/10.3174/ajnr.A7745
http://www.ajnr.org/content/44/1/40

Topological Structural Brain Connectivity Alterations in Aspartylglucosaminuria: A Case-Control Study

U. Roine, A.M. Tokola, T. Autti, and T. Roine

ABSTRACT

BACKGROUND AND PURPOSE: We investigated global and local properties of the structural brain connectivity networks in aspartylglucosaminuria, an autosomal recessive and progressive neurodegenerative lysosomal storage disease. Brain connectivity in aspartylglucosaminuria has not been investigated before, but previous structural MR imaging studies have shown brain atrophy, delayed myelination, and decreased thalamic and increased periventricular WM T2 signal intensity.

MATERIALS AND METHODS: We acquired diffusion MR imaging and T1-weighted data from 12 patients with aspartylglucosaminuria (mean age, 23 [SD, 8] years; 5 men), and 30 healthy controls (mean age, 25 [SD, 10] years; 13 men). We performed whole-brain constrained spherical deconvolution tractography, which enables the reconstruction of neural tracts through regions with complex fiber configurations, and used graph-theoretical analysis to investigate the structural brain connectivity networks.

RESULTS: The integration of the networks was decreased, as demonstrated by a decreased normalized global efficiency and an increased normalized characteristic path length. In addition, the average strength of the networks was decreased. In the local analyses, we found decreased strength in 11 nodes, including, for example, the right thalamus, right putamen, and, bilaterally, several occipital and temporal regions.

CONCLUSIONS: We found global and local structural connectivity alterations in aspartylglucosaminuria. Biomarkers related to the treatment efficacy are needed, and brain network properties may provide the means for long term follow-up.

ABBREVIATION: AGU = aspartylglucosaminuria

Aspartylglucosaminuria (AGU) is a rare, progressive, neurodegenerative lysosomal storage disease. It is inherited in a recessive manner and is caused by a mutation in the aspartylglucosaminidase (*AGA*) gene located in 4q34.3.[1] Due to the isolated population, it has developed in Finland, where the estimated incidence of AGU is 1:18,000 and there are about 160–200 patients with AGU in the country.[2] It has been estimated that 200–300 patients with AGU exist worldwide.[2] More than 30 *AGA* variants have been identified in patients with AGU, but in Finland, 98% of patients have the AGU_{FIN} major variant.[3] The mutations in the *AGA* gene result in deficient activity of a lysosomal hydrolase enzyme called aspartylglucosaminidase, which is responsible for breaking a N-glycosidic bond between carbohydrates and proteins, and this leads to excessive accumulation of uncleaved aspartylglucosamine and other glycoasparagines in tissues.[1,2] With time, AGU affects the whole body, including the CNS, in a progressive manner.

The first neurologic signs are often developmental delays, such as clumsy walking and delayed speech, noticed around 12–15 months of age, and progressive intellectual impairment finally leads to severe intellectual disability.[4] Autistic features, behavioral disturbances, epilepsy, and disrupted sleep patterns may be present.[4] Motor skills also deteriorate with time, and skeletal and connective tissue abnormalities may be present.[4] Typical facial features include macroglossia, thick lips, low and wide nasal bridge, short nose, puffy eyelids, and broad face.[4] After early macrocephaly, the head size reduces, though the

Received March 23, 2022; accepted after revision November 16.

From the Department of Radiology (U.R., A.M.T., T.A., T.R.), HUS Medical Imaging Center, and Department of Pediatric Neurology (U.R.), Children's Hospital, University of Helsinki and Helsinki University Hospital, Helsinki, Finland; Department of Neuroscience and Biomedical Engineering (T.R.), Aalto University School of Science, Espoo, Finland; and Turku Brain and Mind Center (T.R.), University of Turku, Turku, Finland.

T. Autti and T. Roine contributed equally to this work.

U.R. received funding from the Finnish Medical Foundation and the Arvo and Lea Ylppö Foundation. A.M.T. received funding from the Rinnekoti Research Foundation, the Finnish Brain Foundation, and the Arvo and Lea Ylppö Foundation. T.R. received funding from the Finnish Cultural Foundation.

Please address correspondence to Timo Roine, MD, HUS Medical Imaging Center, Radiology, University of Helsinki and Helsinki University Hospital, PL 22 (Haartmaninkatu 4), FI-00014 Helsingin Yliopisto, Finland; e-mail: timo.roine@iki.fi; @TimoRoine

Indicates article with online supplemental data.

http://dx.doi.org/10.3174/ajnr.A7745

skull may be thickened.[5] The disease leads to a premature death, typically before 45 years of age.[6]

The AGU diagnosis is made on the basis of genetic testing, though biochemical tests of accumulated aspartylglucosamine in urine can be useful for screening purposes.[4] No curative therapies currently exist, but several preclinical studies aiming at enzyme replacement or gene therapy have been published,[7-10] and in 2018, a 4-year clinical trial was initiated with a pharmacologic chaperone called betaine.[11] It facilitates the correct folding of aspartylglucosaminidase mutants, because most *AGA* variants cause misfolding of the protein.[4] The benefit of hematopoietic stem cell transplantation is unclear.[4]

With the emerging new treatments, new methods to evaluate the response are needed. Biochemical tests, such as aspartylglucosaminidase enzyme activity, could potentially be used as surrogate biomarkers.[4] MR imaging–based measures, including structural brain connectivity, could provide a means for evaluating the progression of the disease.

Conventional MR imaging studies in AGU have shown brain atrophy, delayed myelination, decreased thalamic T2 signal intensity, and increased T2 signal intensity in the periventricular WM.[12-16] In addition, on the basis of a visual analysis, poor differentiation between white and gray matter, thinning of the corpus callosum, cerebellar atrophy, and mild ventricular dilation have been reported.[14] Representative figures of the abnormalities in conventional MR imaging have been published by Tokola et al.[14] Diffusion MR imaging has been used to study a 10-year-old boy with AGU, and decreased fractional anisotropy was found in the corpus callosum and thalamocortical pulvinar tracts compared with his healthy twin brother.[17]

Possible alterations in structural brain connectivity have not been investigated in AGU. Diffusion MR imaging followed by whole-brain tractography and graph-theoretical methods can be used to reliably study the whole-brain connectivity in health and disease.[18-21] The association of structural brain connectivity with the response to medication has also been studied, for example, in bipolar disorder and schizophrenia.[22,23] The aim of the current study was to recognize possible global or local abnormalities in the structural brain connectivity networks in patients with AGU compared with healthy controls. On the basis of the findings in another lysosomal storage disease,[24] juvenile neuronal ceroid lipofuscinosis, we expected to find globally decreased integration of the structural brain connectivity networks in AGU. In addition, we expected to find several local alterations in the connectivity based on the wide spectrum of the symptoms.

MATERIALS AND METHODS

In summary, we performed whole-brain tractography on the basis of diffusion MR imaging data to reconstruct the WM tracts in the brain and segmented the GM of the brain into 164 anatomic regions. Then, we reconstructed structural brain connectivity networks by assigning each end of the reconstructed fiber tracts to corresponding segmented anatomic regions and used graph-theoretical methods to investigate the global and local properties in the structural brain connectivity networks of patients with AGU and healthy controls.

Participants

Twelve patients with AGU, mean age, 23 years 11 months (SD, 8 years 3 months) (range, 9–35 years; 5 males) and 30 healthy age- and sex-matched controls, mean age, 25 years 5 months (SD, 9 years 11 months) (range, 9–46 years; 13 males), participated in this study. Due to the rarity of the disease, we were not able to recruit more patients. Two-way *t* tests with a significance threshold $\alpha < .05$ were used to determine sufficient age- and sex-matching of the two groups. All patients were diagnosed using a urine test showing elevated levels of apartylglucosamine and a blood test showing deficiency in the *AGA* enzyme. The control subjects were healthy volunteers recruited from the Helsinki and Uusimaa region who had no neurologic, psychiatric, or other major diagnoses or medications. All participants and/or their parents gave informed consent before the study, which was approved by the local ethics committee of the Hospital District of Helsinki and Uusimaa (ethics permission, 247/E7/2007).

MR Imaging Acquisition

The MR imaging data were acquired with an Achieva 3T machine (Phillips Healthcare) at the Helsinki University Hospital, Finland, from 2007 to 2012. Sedation was not used during the scanning due to ethical reasons. T1 3D axial series were acquired with $1 \times 1 \times 1$ mm resolution (TR = 68.15 ms, TE = 3.75 ms, matrix size = 256×256 mm, flip angle = 8°). Two radiologists visually evaluated the conventional sequences, and the findings have been reported previously.[14] For the single-shot axial diffusion-weighted data, 32 gradient orientations, a diffusion-weighting = 1000 s/mm^2, TR = 10,809 ms, TE = 59.5 ms, FOV = 224×224 mm, and an isotropic 2-mm voxel size was used. One image was acquired with no diffusion-weighting.

Reconstruction of the Structural Brain Connectivity Networks

First, the data were corrected for motion-[25] and eddy current–induced distortions in ExploreDTI (https://www.exploredti.com/).[26] Because no reverse phase-encoding data were available, echo-planar imaging distortions were corrected via nonlinear registration with cubic b-splines to the T1-weighted data.[27] Then, we performed constrained spherical deconvolution based whole-brain streamline tractography, which enables the reconstruction of neural tracts through regions with complex WM configurations, such as crossing fibers.[28,29] Next, we segmented 164 cortical and subcortical GM areas from the T1-weighted images using FreeSurfer (http://surfer.nmr.mgh.harvard.edu).[30,31] The validity of the segmentations was visually confirmed for all subjects. Finally, we reconstructed structural brain connectivity networks, connectomes, by assigning the reconstructed streamline tracts to the GM areas on the basis of their end points.[18,19] These GM areas became the nodes of the network, and the edges between the nodes were weighted by the number of the reconstructed tracts between each pair of areas, resulting in a 164×164 connectivity matrix. The reconstruction of structural brain connectivity networks is presented in Fig 1.

Graph-Theoretical Analyses

Graph-theoretical analyses were performed with the Brain Connectivity Toolbox in Matlab (MathWorks).[32] We investigated

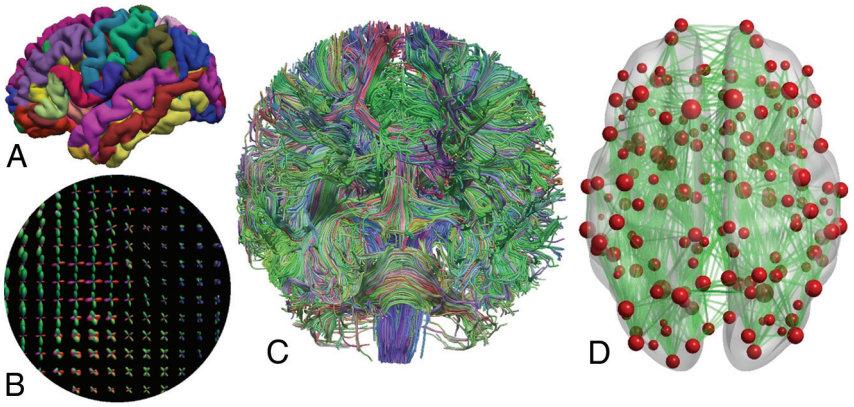

FIG 1. Reconstruction of structural brain connectivity networks. *A*, Cortical and subcortical GM was parcellated into 164 regions based on the T1-weighted images. *B*, Constrained spherical deconvolution was used to estimate complex fiber orientation distributions from diffusion MR imaging data. *C*, Whole-brain probabilistic streamline tractography was performed to reconstruct (*D*) structural brain connectivity networks, in which nodes represent GM regions and the edges between the nodes represent the WM connectivity (number of streamlines) between the regions. The size of the nodes corresponds to the strength of the node, and the opacity of the edges is scaled according to the number of streamlines. The fiber orientation distributions and whole-brain tractography are colored according to the directions in the brain: red (left-right), blue (superior-inferior), and green (anterior-posterior).

7 global (betweenness centrality, normalized clustering coefficient, normalized global efficiency, normalized characteristic path length, small-worldness, degree, and strength) and 3 local (betweenness centrality, efficiency, and strength) properties of the structural connectome.[19] These properties were compared between the patients with AGU and the control subjects. In addition, the correlations of the global properties with age were also investigated both in patients with AGU and controls.

Statistical Analyses

Statistical analyses were performed in SPSS Statistics, Version 27 (IBM). Age and sex were used as covariates in all analyses except for the correlation analyses between the global network properties and age. There were no missing data. The Bonferroni correction was used to correct for the family-wise error rate using $n = 7$ for the global analyses and $n = 164$ for the local node-level analyses. Due to the small sample size, the assumptions of normality and homogeneity of variances for the F tests were rigorously checked for each variable, and whenever the assumptions were not met, a nonparametric Mann-Whitney U test (2-sided, corrected for ties) was used instead.[33] However, because the covariates cannot be taken into account in the nonparametric test, we chose to report only the findings that were significant using both approaches.

Scientific Visualizations

BrainNet Viewer (https://www.nitrc.org/projects/bnv/),[34] MRtrix3 (https://www.mrtrix.org/),[35] seaborn (https://seaborn.pydata.org/),[36] and Matplotlib (https://matplotlib.org/)[37] were used to produce the scientific visualizations.

RESULTS

We investigated both global and local properties of the structural connectome in patients with AGU compared with control subjects. Of the global properties, small-worldness ($F = 11.6$, $P = .0006$), strength ($F = 15.9$, $P = .0003$), degree ($F = 8.4$, $P = .006$), and normalized global efficiency ($F = 15.5$, $P = .0003$) were significantly decreased, and characteristic path length was significantly increased ($F = 35.9$, $P = .0000006$) in AGU after Bonferroni correction for multiple comparisons, as demonstrated in Fig 2. The results, except for node degree, also remained significant without using age and sex as covariates. However, when taking into account the assumptions of the F tests, normality and homoscedasticity, the differences in small-worldness and degree were not statistically significant in the nonparametric Mann-Whitney U tests.

We also investigated the correlation between the global properties and age in both the patients and controls. As shown in Fig 3, the normalized clustering coefficient and average strength decreased with age in both patients with AGU and control subjects while being lower at all ages in AGU. Moreover, in characteristic path length, global efficiency, small-worldness, and degree, the differences between the 2 groups were smaller in the younger subjects and increased with age.

In the local node-level analyses, we found decreased strength in 12 nodes using F tests and age and sex as covariates. In 11 of these nodes, the strength was also significantly decreased using a nonparametric Mann-Whitney U test performed without using age and sex as covariates whenever the assumptions of the F test were not met. These regions included the right thalamus, right putamen, and several nodes in the occipital and temporal regions in both hemispheres, shown in Fig 4 and the Online Supplemental Data. Local efficiency or betweenness centrality were not affected. The results were corrected for multiple comparisons using a Bonferroni-corrected significance threshold of $P < .05/164 = .0003$. The complete node-level results are presented in the Online Supplemental Data.

DISCUSSION

The purpose of our study was to investigate whether there are global or local abnormalities in the structural brain connectivity networks in patients with AGU. First, we performed whole-brain tractography to reconstruct the WM tracts in the brain, then we segmented the GM into 164 anatomic areas, and finally, we reconstructed structural brain networks, which we analyzed by using graph-theoretical tools. We found both global and local topological alterations in the brain connectivity in patients with AGU compared with the control group. In addition, we observed an altered age relationship in patients with AGU.

To investigate the integration of the networks, we calculated normalized global efficiency[38] and normalized characteristic path length,[39] which both showed decreased integration in patients with AGU. Characteristic path length is primarily affected by longer paths; global efficiency, by shorter paths. Thus, our results

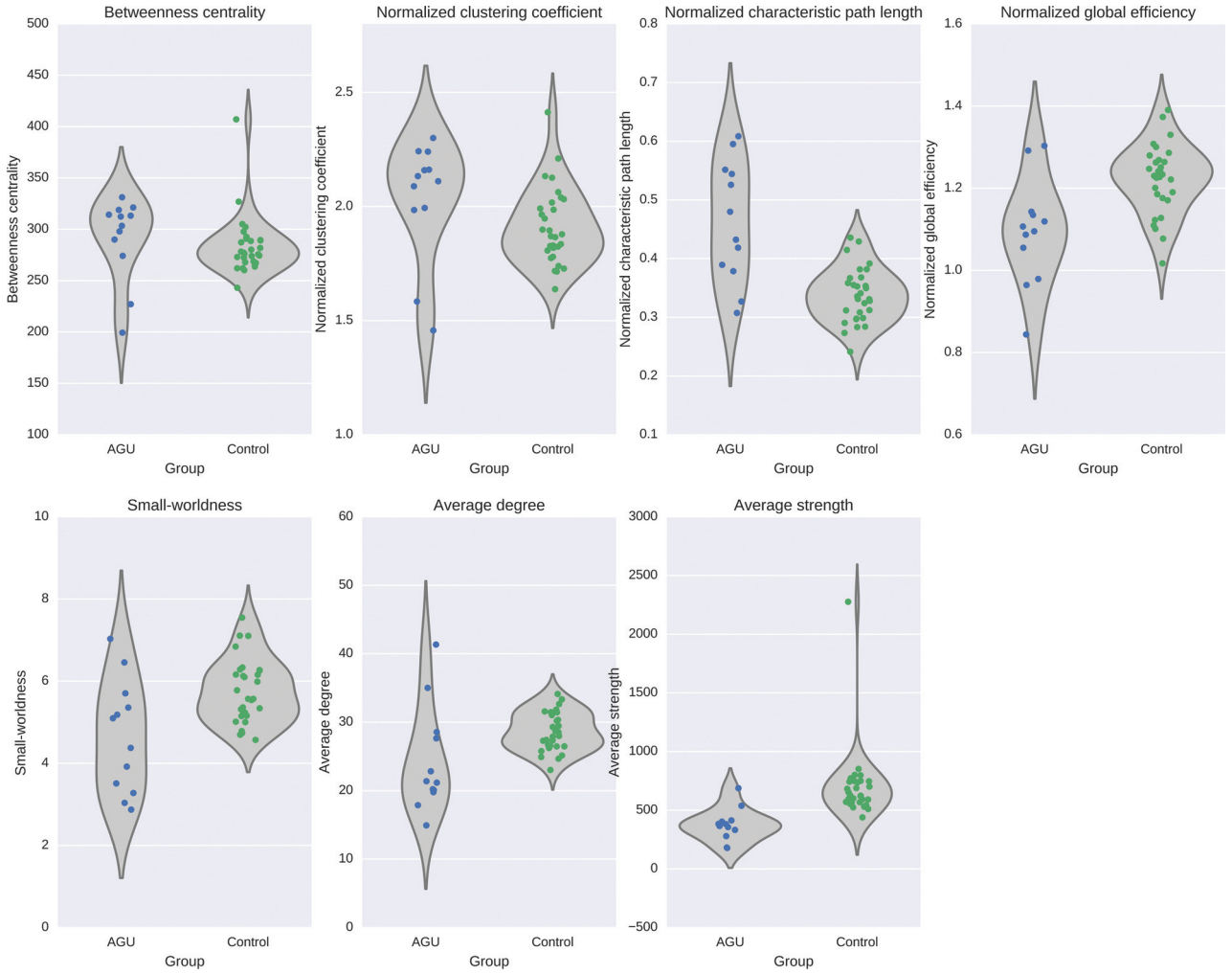

FIG 2. Global graph theoretical properties of the structural brain connectivity networks in patients with AGU and control subjects. The *violin plots* show the full distribution of the data via kernel density plots.

suggest that alterations in both shorter and longer paths are present in patients with AGU compared with control subjects.

We investigated the segregation of the brain networks using the normalized clustering coefficient,[40] which measures the fraction of triangles formed by neighboring nodes compared with all possible triangles between them. However, no differences were found in the normalized clustering coefficient between patients with AGU and control subjects. Finally, the average strength was decreased in the brain networks of patients with AGU, suggesting overall decreased global connectivity in AGU.

The development and organization of brain circuitry require coordination of a complex set of neurodevelopmental events, which may be disturbed in AGU. We know that myelination is delayed and deficient in AGU, the volume of WM is decreased in school-aged children even in visual evaluation, and general atrophy is slowly progressive during the following years.[15,41,42] Vacuolation of neurons and neuronal loss have been reported in neuropathologic studies among patients with AGU with advanced disease.[15] The delayed and deficient myelination and neuronal loss may disturb synaptogenesis as well as pruning, resulting in impaired integration of networks. Furthermore, accumulation of iron in the thalamic nuclei in AGU, which has been shown with susceptibility-weighted imaging in school-aged patients,[43,44] may disturb the connectivity of various thalamic circuits. The relationship between iron concentration and structural connectivity has not been thoroughly investigated, but in one study, significant correlations between the iron levels of the subthalamic nuclei and the number of WM tracts terminating in different GM areas were shown in patients with Parkinson disease.[45] In another study, higher cortical iron concentration was associated with lower (task-based) functional connectivity within a frontoparietal working memory network and with poorer working memory performance.[46]

In the local analyses, we found decreased strength in 12 GM areas, of which 11 were also significant when a nonparametric Mann-Whitney *U* test was used whenever the assumptions of the *F* tests were not met. These included the right thalamus and putamen, which have previously been shown to have a decreased T2-weighted signal intensity in AGU.[14] In addition, the strengths of the left thalamus ($P = .003$) and left putamen ($P = .002$) were decreased but did not endure correction for multiple comparisons (Online Supplemental Data). We also found decreased

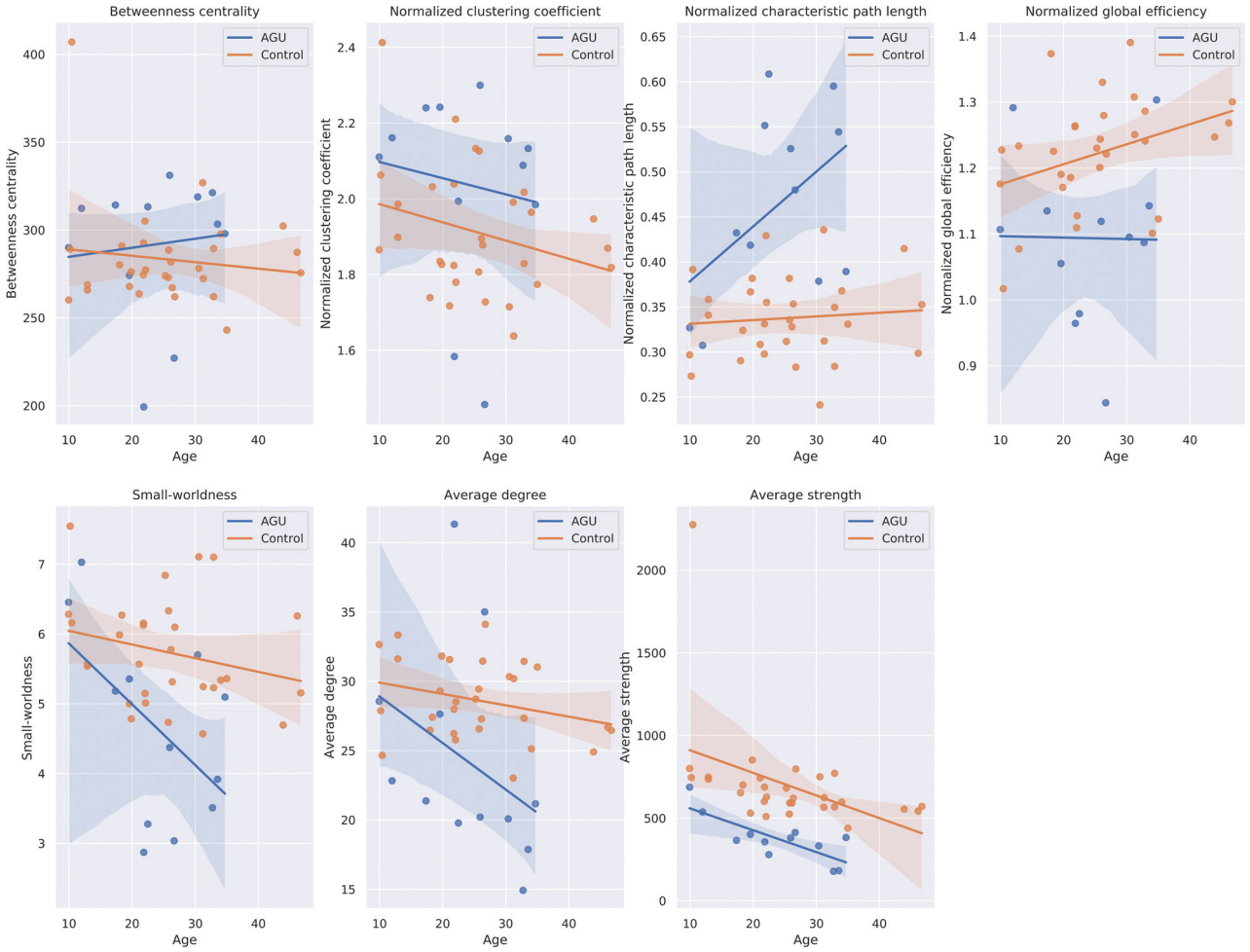

FIG 3. Correlation of the global network properties with age in patients with AGU and control subjects. The *shaded area* shows the 95% confidence interval for the regression lines.

strength bilaterally in the middle temporal gyri, responsible for recognition of known faces and accessing word meaning while reading,[47] and in the left planum temporale, a highly lateralized structure overlapping with the Wernicke area and involved in early auditory processing including language and music.[48-50] Its symmetric development has been related to dyslexia[51] and stuttering.[52] The decrease in the strength of the left planum temporale found in this study may indicate increased symmetry in AGU.

We have also recently investigated the WM abnormalities in another lysosomal storage disease, juvenile neuronal ceroid lipofuscinosis (lysosomal/endosomal transmembrane protein, battenin [CLN3]). In the microstructural analyses, we found globally decreased anisotropy and increased diffusivity in patients with CLN3 compared with controls.[53] Locally, we found decreased anisotropy and increased diffusivity in the corona radiata and posterior thalamic radiation. We also found significant global and local network alterations that correlated with the disease severity in CLN3, including significantly decreased integration and degree of the structural brain networks.[24] Consistent findings in these lysosomal storage diseases may indicate that integration of the structural brain networks is decreased in lysosomal storage diseases in general. Moreover, the local network properties of the left planum temporale were affected in both AGU and CLN3.

Limitations of this study include the small sample size and suboptimal acquisition parameters (low b-value and number of gradient orientations).[54] However, AGU is a rare disease, and larger sample sizes are difficult to collect. Unfortunately, we do not have sufficient clinical data for these patients available; therefore, although it would have increased the clinical importance of our findings, we could not perform any correlation analyses between the brain connectivity metrics and clinical variables. Although we carefully verified the success of the segmentations for each subject, we did not account for conventional MR imaging findings or WM hyperintensities in the statistical analyses.

In the future, we would recommend using higher diffusion-weighting with multiple b-values to be able to investigate more specific properties of the WM tracts such as fiber density.[55] Furthermore, the relationship among the properties of the structural brain connectivity networks, iron accumulation, and clinical variables such as disease severity should be investigated. Finally, biomarkers for treatment efficacy are needed, and structural connectivity network analysis may provide means for long-term follow-up.

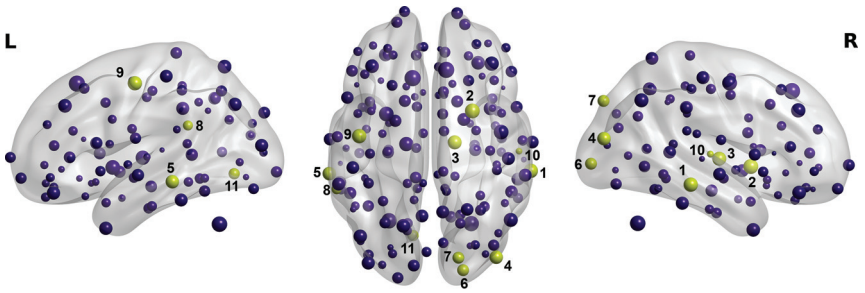

FIG 4. Local alterations in the strength of the structural brain connectivity networks in AGU compared with control subjects. Decreased strength of the structural brain connectivity networks in AGU compared with control subjects was found in 11 nodes (Online Supplemental Data), shown in yellow: 1) right middle temporal gyrus, 2) right putamen, 3) right thalamus, 4) right middle occipital gyrus, 5) left middle temporal gyrus, 6) right occipital pole, 7) right superior occipital gyrus, 8) left planum temporale, 9) left precentral gyrus, 10) right transverse temporal gyrus, and 11) left lingual gyrus. These results endured the Bonferroni correction for multiple comparisons. The size of the nodes corresponds to their strength. The complete results are presented in the Online Supplemental Data.

CONCLUSIONS

We investigated the graph-theoretical properties of the structural brain connectivity networks in AGU and found highly significant global topological alterations such as decreased integration of the networks in AGU. In addition, we found decreased strength in 11 regions, including the right thalamus and putamen, previously also found to be affected in conventional MR imaging studies of AGU. Our results may also be helpful in planning studies concerning other neurodegenerative diseases.

Disclosure forms provided by the authors are available with the full text and PDF of this article at www.ajnr.org.

REFERENCES

1. Saarela J, von SC, Peltonen L, et al. **A novel aspartylglucosaminuria mutation affects translocation of aspartylglucosaminidase.** *Hum Mutat* 2004;24:350–51 CrossRef Medline
2. Arvio M, Mononen I. **Aspartylglycosaminuria: a review.** *Orphanet J Rare Dis* 2016;11:162 CrossRef Medline
3. Syvänen AC, Ikonen E, Manninen T, et al. **Convenient and quantitative determination of the frequency of a mutant allele using solid-phase minisequencing: application to aspartylglucosaminuria in Finland.** *Genomics* 1992;12:590–95 CrossRef Medline
4. Goodspeed K, Feng C, Laine M, et al. **Aspartylglucosaminuria: clinical presentation and potential therapies.** *J Child Neurol* 2021;36:403–14 CrossRef Medline
5. Arvio M, Arvio P, Hurmerinta K, et al. **Reduction in head size in patients with aspartylglucosaminuria.** *Acta Neurol Scand* 2005;112:335–37 CrossRef Medline
6. Arvio P, Arvio M. **Progressive nature of aspartylglucosaminuria.** *Acta Paediatr* 2007;91:255–57 CrossRef Medline
7. Dunder U, Valtonen P, Kelo E, et al. **Early initiation of enzyme replacement therapy improves metabolic correction in the brain tissue of aspartylglycosaminuria mice.** *J Inherit Metab Dis* 2010;33:611–17 CrossRef Medline
8. Kelo E, Dunder U, Mononen I. **Massive accumulation of Man2GlcNAc2-Asn in nonneuronal tissues of glycosylasparaginase-deficient mice and its removal by enzyme replacement therapy.** *Glycobiology* 2005;15:79–85 CrossRef Medline
9. Peltola M, Kyttälä A, Heinonen O, et al. **Adenovirus-mediated gene transfer results in decreased lysosomal storage in brain and total correction in liver of aspartylglucosaminuria (AGU) mouse.** *Gene Ther* 1998;5:1314–21 CrossRef Medline
10. Virta S, Rapola J, Jalanko A, et al. **Use of nonviral promoters in adenovirus-mediated gene therapy: reduction of lysosomal storage in the aspartylglucosaminuria mouse.** *J Gene Med* 2006;8:699–706 CrossRef Medline
11. Banning A, Gülec C, Rouvinen J, et al. **Identification of small molecule compounds for pharmacological chaperone therapy of aspartylglucosaminuria.** *Sci Rep* 2016;6:37583 CrossRef Medline
12. Autti T, Joensuu R, Åberg L. **Decreased T2 signal in the thalami may be a sign of lysosomal storage disease.** *Neuroradiology* 2007;49:571–78 CrossRef Medline
13. Autti T, Lönnqvist T, Joensuu R. **Bilateral pulvinar signal intensity decrease on T2-weighted images in patients with aspartylglucosaminuria.** *Acta Radiol* 2008;49:687–92 CrossRef Medline
14. Tokola A, Åberg L, Autti T. **Brain MRI findings in aspartylglucosaminuria.** *J Neuroradiol* 2015;42:345–57 CrossRef Medline
15. Autti T, Raininko R, Haltia M, et al. **Aspartylglucosaminuria: radiologic course of the disease with histopathologic correlation.** *J Child Neurol* 1997;12:369–75 CrossRef Medline
16. Goodspeed K, Horton D, Lowden A, et al. **A cross-sectional natural history study of aspartylglucosaminuria.** *JIMD Rep* 2022;63:425–33 CrossRef Medline
17. Tokola A, Brandstack N, Hakkarainen A, et al. **White matter microstructure and subcortical gray matter structure volumes in aspartylglucosaminuria; a 5-year follow-up brain MRI study of an adolescent with aspartylglucosaminuria and his healthy twin brother.** *JIMD Rep* 2017;35:105–15 CrossRef Medline
18. Hagmann P, Cammoun L, Gigandet X, et al. **Mapping the structural core of human cerebral cortex.** *PLoS Biol* 2008;6:e159–93 CrossRef Medline
19. Bullmore E, Sporns O. **Complex brain networks: graph theoretical analysis of structural and functional systems.** *Nat Rev Neurosci* 2009;10:186–98 CrossRef Medline
20. Griffa A, Baumann PS, Thiran JP, et al. **Structural connectomics in brain diseases.** *Neuroimage* 2013;80:515–26 CrossRef Medline
21. Roine T, Jeurissen B, Perrone D, et al. **Reproducibility and intercorrelation of graph theoretical measures in structural brain connectivity networks.** *Med Image Anal* 2019;52:56–67 CrossRef Medline
22. Lei D, Li W, Tallman MJ, et al. **Changes in the brain structural connectome after a prospective randomized clinical trial of lithium and quetiapine treatment in youth with bipolar disorder.** *Neuropsychopharmacology* 2021;46:1315–23 CrossRef Medline
23. Hu M, Zong X, Zheng J, et al. **Risperidone-induced topological alterations of anatomical brain network in first-episode drug-naive schizophrenia patients: a longitudinal diffusion tensor imaging study.** *Psychol Med* 2016;46:2549–60 CrossRef Medline
24. Roine T, Roine U, Tokola A, et al. **Topological alterations of the structural brain connectivity network in children with juvenile neuronal ceroid lipofuscinosis.** *AJNR Am J Neuroradiol* 2019;40:2146–53 CrossRef Medline
25. Leemans A, Jones DK. **The B-matrix must be rotated when correcting for subject motion in DTI data.** *Magn Reson Med* 2009;61:1336–49 CrossRef Medline
26. Leemans A, Jeurissen B, Sijbers J, et al. **ExploreDTI: a graphical toolbox for processing, analyzing, and visualizing diffusion MR data.** January 2009. In: *Proceedings of the 17th Annual Meeting of the International Society for Magnetic Resonance in Medicine*, 2009;3537
27. Irfanoglu MO, Walker L, Sarlls J, et al. **Effects of image distortions originating from susceptibility variations and concomitant fields**

on diffusion MRI tractography results. *Neuroimage* 2012;61:275–88 CrossRef Medline
28. Jeurissen B, Leemans A, Jones DK, et al. **Probabilistic fiber tracking using the residual bootstrap with constrained spherical deconvolution.** *Hum Brain Mapp* 2011;32:461–79 CrossRef Medline
29. Tournier JD, Calamante F, Connelly A. **Robust determination of the fibre orientation distribution in diffusion MRI: non-negativity constrained super-resolved spherical deconvolution.** *Neuroimage* 2007;35:1459–72 CrossRef Medline
30. Destrieux C, Fischl B, Dale A, et al. **Automatic parcellation of human cortical gyri and sulci using standard anatomical nomenclature.** *Neuroimage* 2010;53:1–15 CrossRef Medline
31. Fischl B. **FreeSurfer.** *Neuroimage* 2012;62:774–81 CrossRef Medline
32. Rubinov M, Sporns O. **Complex network measures of brain connectivity: uses and interpretations.** *Neuroimage* 2010;52:1059–69 CrossRef Medline
33. Mann HB, Whitney DR. **On a test of whether one of two random variables is stochastically larger than the other.** *Ann Math Stat* 1947;18:50–60 CrossRef
34. Xia M, Wang J, He Y. **BrainNet Viewer: a network visualization tool for human brain connectomics.** *PLoS One* 2013;8:e68910 CrossRef Medline
35. Tournier JD, Smith R, Raffelt D, et al. **MRtrix3: a fast, flexible and open software framework for medical image processing and visualisation.** *Neuroimage* 2019;202:116137 CrossRef Medline
36. Waskom M. **Seaborn: statistical data visualization.** *J Open Source Softw*. 2021;6:3021 CrossRef
37. Hunter JD. **Matplotlib: a 2D graphics environment.** *Comput Sci Eng* 2007;9:90–95 CrossRef
38. Latora V, Marchiori M. **Efficient behavior of small-world networks.** *Phys Rev Lett* 2001;87:198701 CrossRef Medline
39. Watts DJ, Strogatz SH. **Collective dynamics of "small-world" networks.** *Nature* 1998;393:440–42 CrossRef Medline
40. Saramäki J, Kivelä M, Onnela JP, et al. **Generalizations of the clustering coefficient to weighted complex networks.** *Phys Rev E Stat Nonlin Soft Matter Phys.*2007;75(2 Pt 2):027105 CrossRef Medline
41. Arstila A, Palo J, Haltia M, et al. **Aspartylglucosaminuria I: fine structural studies on liver, kidney and brain.** *Acta Neuropathol* 1972;20:207–16 CrossRef Medline
42. Haltia M, Palo J, Autio S. **Aspartylglycosaminuria: a generalized storage disease.** *Acta Neuropathol* 1975;31:243–55 CrossRef Medline
43. Tokola A, Laine M, Tikkanen R, et al. **Susceptibility-weighted imaging findings in aspartylglucosaminuria.** *AJNR Am J Neuroradiol* 2019;40:1850–54 CrossRef Medline
44. Sairanen V, Tokola A, Tikkanen R, et al. **Statistical permutation test reveals progressive and region-specific iron accumulation in the thalami of children with aspartylglucosaminuria.** *Brain Sci* 2020;10:677 CrossRef Medline
45. Dimov A, Patel W, Yao Y, et al. **Iron concentration linked to structural connectivity in the subthalamic nucleus: implications for deep brain stimulation.** *J Neurosurg* 2019 Jan 18. [Epub head of print] CrossRef Medline
46. Zachariou V, Bauer CE, Seago ER, et al. **Cortical iron disrupts functional connectivity networks supporting working memory performance in older adults.** *Neuroimage* 2020;223:117309 CrossRef Medline
47. Acheson DJ, Hagoort P. **Stimulating the brain's language network: syntactic ambiguity resolution after TMS to the inferior frontal gyrus and middle temporal gyrus.** *J Cogn Neurosci* 2013;25:1664–77 CrossRef
48. Binder JR, Frost JA, Hammeke TA, et al. **Function of the left planum temporale in auditory and linguistic processing.** *Brain* 1996;119:1239–47 CrossRef Medline
49. Keenan JP, Thangaraj V, Halpern AR, et al. **Absolute pitch and planum temporale.** *Neuroimage* 2001;14:1402–08 CrossRef Medline
50. Dorsaint-Pierre R, Penhune VB, Watkins KE, et al. **Asymmetries of the planum temporale and Heschl's gyrus: relationship to language lateralization.** *Brain* 2006;129:1164–76 CrossRef Medline
51. Larsen JP, Høien T, Lundberg I, et al. **MRI evaluation of the size and symmetry of the planum temporale in adolescents with developmental dyslexia.** *Brain Lang* 1990;39:289–301 CrossRef Medline
52. Foundas AL, Bollich AM, Feldman J, et al. **Aberrant auditory processing and atypical planum temporale in developmental stuttering.** *Neurology* 2004;63:1640–46 CrossRef Medline
53. Roine U, Roine T, Hakkarainen A, et al. **Global and widespread local white matter abnormalities in juvenile neuronal ceroid lipofuscinosis.** *AJNR Am J Neuroradiol* 2018;39:1349–54 CrossRef Medline
54. Tournier JD, Calamante F, Connelly A. **Determination of the appropriate b value and number of gradient directions for high-angular-resolution diffusion-weighted imaging.** *NMR Biomed* 2013;26:1775–86 CrossRef Medline
55. Raffelt D, Tournier JD, Rose S, et al. **Apparent fibre density: a novel measure for the analysis of diffusion-weighted magnetic resonance images.** *Neuroimage* 2012;59:3976–94 CrossRef Medline